Dalton Transactions

RSC Publishing

PAPER

View Article Online
View Journal | View Issue

Cite this: *Dalton Trans.*, 2013, **42**, 4059

Synthesis, characterization and electrochemiluminescent properties of cyclometalated platinum(II) complexes with substituted 2-phenylpyridine ligands†

Chunxiang Li,*[a] Shuqin Wang,[a] Yangmei Huang,[a] Bin Zheng,[a] Ziqi Tian,[c] Yonghong Wen[a] and Feng Li*[b]

Two neutral cyclometalated platinum(II) complexes, Pt(DPP)(acac) and Pt(BPP)(acac) (DPP = 2,4-diphenylpyridine, BPP = 2-(4-*tert*-butylphenyl)-4-phenylpyridine, acac = acetylacetone), have been synthesized and characterized by ^{1}H NMR spectroscopy, mass spectrometry, elemental analyses and by X-ray crystallography for Pt(DPP)(acac). Electrogenerated chemiluminescence (ECL) of the two complexes in the absence or presence of coreactant tri-*n*-propylamine (TPrA) in different solvents (CH_3CN, CH_2Cl_2, DMF, CH_3CN/H_2O (V, 50 : 50)) has been studied. The ECL spectra are identical to their own PL spectra, indicating that ECL processes lead to the same metal-to-ligand charge-transfer (^{3}MLCT) excited state that is generated by light excitation. The ECL potentials of Pt(DPP)(acac) and Pt(BPP)(acac)/TPrA in CH_3CN and CH_3CN/H_2O solution were at ~0.75 V *vs.* SCE, and significantly negatively shifted by about 0.6 V compared to that of the $Ru(bpy)_3^{2+}$/TPrA system. The ECL quantum efficiencies of the complexes are comparable to that of the $Ru(bpy)_3^{2+}$/TPrA system. The significant increase of the ECL signal in the coreactant system is due to the formation of the strongly reducing intermediate TPrA$^{\cdot}$. It is noteworthy that the ECL efficiencies of the synthesized compounds are much higher than that of the tridentate polypyridyl ligands.

Received 17th October 2012,
Accepted 18th December 2012

DOI: 10.1039/c2dt32466k

www.rsc.org/dalton

Introduction

Electrogenerated chemiluminescence (ECL) has now become a very powerful analytical technique and been widely used in immunoassays, DNA analyses and food and water testing, because of its inherent features, such as low background, high sensitivity, good reproducibility and selectivity.[1–4] These applications are predominantly based on the fundamental ECL research work of a variety of ECL-active reagents. The design and synthesis of new excellent ECL luminophores have attracted considerable interest since Bard *et al.* reported the first ECL from the $Ru(bpy)_3$(tris-(2,2′-bipyridyl) ruthenium(II))/tri-*n*-propylamine (TPrA) system.[3,5–7] In the past several years, a number of organometallic complexes such as Al(III), Re(I), Ir(III), Os(II), Eu(II) and Pt(II) complexes have been studied as new ECL reagents due to their thermal and photochemical stability and high photoluminescence.[8–13]

Recently, luminescent square-planar platinum(II) complexes have gained major attention because of their extensive applications in many fields, such as chemosensors, photocatalysis and organic light-emitting diodes (OLEDs) in view of their rich photoluminescence properties.[14–18] The strong spin–orbit coupling of the heavy metal atom allows for efficient intersystem crossing (ISC) between singlet and triplet states, which can lead to a high quantum yield of emission from the triplet state. Meanwhile, the electrochemistry properties of platinum(II) complexes have been studied, which revealed well-defined redox behaviors.[19,20] Effective ECL from the homoleptic $Pt(Thpy)_2$ complex (Thpy = 2-(2-thienyl)-2-pyridine) has also been demonstrated by Balzani *et al.* in coreactant systems.[21] Recent studies on the ECL of platinum(II) complexes were focused on complexes containing tridentate polypyridyl ligands,[12,22–26] while the ECL properties of heteroleptic (*C*^*N*)-Pt(LX) complexes (*C*^*N* represents a cyclometalating ligand and LX represents an ancillary ligand) have not been studied so far, although many exhibit more excellent

[a]*State Key Laboratory Base of Eco-chemical Engineering, College of Chemistry and Molecular Engineering, Qingdao University of Science and Technology, Qingdao 266042, PR China. E-mail: lichunxiang76@yahoo.com.cn; Tel: +86-532-84022681*
[b]*College of Chemistry and Pharmacy, Qingdao Agricultural University, 700 Changcheng Road, Qingdao 266109, PR China. E-mail: lifeng@qust.edu.cn; Fax: +86-532-86080213; Tel: +86-532-86080213*
[c]*School of Chemistry and Chemical Engineering, Nanjing University, Nanjing, 210093, PR China*

†CCDC reference number 901672. For crystallographic data in CIF or other electronic format see DOI: 10.1039/c2dt32466k

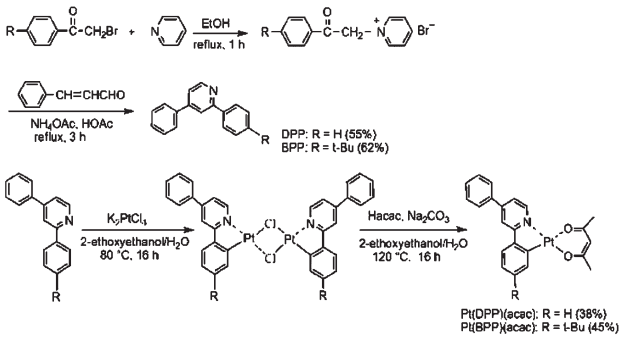

Scheme 1 Synthesis of Pt(DPP)(acac) and Pt(BPP)(acac).

photoluminescence and more tailorable properties than other platinum(II) complexes.

In this paper, two neutral cyclometalated heteroleptic platinum(II) complexes, Pt(DPP)(acac) and Pt(BPP)(acac) (DPP = 2,4-diphenylpyridine, BPP = 2-(4-*tert*-butylphenyl)-4-phenylpyridine, acac = acetylacetone) (as shown in Scheme 1), were synthesized and characterized. Their photophysical properties and ECL characteristics in the absence or presence of coreactant TPrA were evaluated. The ECL intensity of the platinum(II) complexes/TPrA system was found to be a function of the TPrA concentration and is affected by experimental factors, such as the nature of the solvent and pH. The possible pathway for the ECL of the platinum(II) complexes/TPrA system was also proposed.

Experimental

Materials

The cyclometalated ligands 2,4-diphenylpyridine (DPP) and 2-(4-*tert*-butylphenyl)-4-phenylpyridine (BPP) were prepared according to the literature procedure.[27,28] K_2PtCl_4, tetra-*n*-butylammoniumhexafluorophosphate (Bu_4NPF_6), tripropylamine (TPrA) and 2-ethoxyethanol were purchased from Aldrich and used without further purification. Other chemicals and solvents were all of reagent grade for synthesis and used as received. Solvents were purified and distilled using standard procedures. All the aqueous solutions were prepared with deionized water (Milli-Q, Millipore). The pH of the phosphate buffer solution (PBS, 0.1 M) was adjusted with concentrated NaOH or hydrochloric acid.

Synthesis

The synthesis of the platinum(II) complexes was carried out in an inert gas atmosphere despite the air stability of the complexes, the main concern being the oxidative and thermal stability of intermediates at the high temperatures in the reactions. The Pt(II)-dichloro-bridged dimers were prepared using a modified method of that reported by Lewis *et al.*[29] This involves heating the K_2PtCl_4 salt with 2–2.2 equiv. of cyclometalating ligand (DPP or BPP) in a 3 : 1 mixture of 2-ethoxyethanol and water to 80 °C for 16 h. The dimers were isolated in water and were subsequently reacted with 3 equiv. of the acetylacetone ancillary ligand and 10 equiv. of Na_2CO_3 in 2-ethoxyethanol at 120 °C for 16 h. The solvent was removed under reduced pressure, and the compound was purified by flash chromatography using dichloromethane. Subsequently, the product was recrystallized with dichloromethane/methanol.

Pt(DPP)(acac), yellowish green, yield: 38%. ^{1}H NMR ($CDCl_3$, 300 MHz) δ: 9.02 (d, J = 6.1 Hz,1H), 7.81 (s, 1H), 7.74 (d, J = 5.7 Hz, 2H), 7.67 (d, J = 7.2 Hz, 2H), 7.53–7.56 (m, 4H), 7.24 (m, 1H), 7.15 (t, 1H), 5.50 (s, 1H), 2.0 (s, 6H). MS (EI) m/z: 523.8 (8.11, M^+), 424.2 (9.73), 230.7 (45.10), 153.8 (4.65), 84.8 (30.11), 42.9 (100). Anal. Calcd for $C_{22}H_{19}NO_2Pt$: C, 50.38; H, 3.65; N, 2.67. Found: C, 50.69; H, 3.78; N, 2.55. IR (KBr, cm^{-1}): 3436 (vw), 3040 (vw), 1618 (s), 1561 (s), 1514 (s), 1480 (m), 1389 (s), 1270 (m), 1020 (w).

Pt(BPP)(acac), yellow, yield: 45%. ^{1}H NMR ($CDCl_3$, 300 MHz): δ 8.97 (d, J = 6.2 Hz, 1H), 7.69–7.76 (m 5H), 7.55 (d, J = 7.0 Hz, 3H), 7.48 (d, J = 8.2 Hz, 1H), 7.19 (d, J = 8.1 Hz, 1H), 5.50 (s, 1H), 2.0 (s, 6H), 2.4 (s, 9H). MS (EI) m/z: 580.0 (7.69, M^+), 272.0 (5.94), 84.9 (16.7), 63.9 (22.5), 43.9 (100). Anal. Calcd for $C_{26}H_{27}NO_2Pt$: C, 53.78; H, 4.68; N, 2.41. Found: C, 53.69; H, 4.78; N, 2.35. IR (KBr, cm^{-1}): 3444 (w), 3047 (w), 2954 (m), 2859 (w), 1619 (m), 1579 (s), 1517 (m), 1403 (m), 1270 (m), 1022 (w).

X-ray crystallography

A suitable crystal of the Pt(DPP)(acac) complex was obtained by slow evaporation of the CH_2Cl_2–isobutanol solution at room temperature. Single crystal X-ray diffraction data of the complex were collected using a Bruker SMART 1000 CCD diffactometer with graphite monochromated Mo Kα radiation (λ = 0.71073 Å) using the ω scan mode at 298(2) K. Intensity data were corrected for *Lp* factors and empirical absorption. The structure was solved by direct methods and expanded by using Fourier differential techniques with SHELXTL.[30] All non-hydrogen atoms were located with successive difference Fourier syntheses. The hydrogen atoms were geometrically fixed and allowed to ride on the parent atoms to which they are attached. The structure was refined by full-matrix least-squares method on F^2 with anisotropic thermal parameters for all non-hydrogen atoms. Atomic scattering factors and anomalous dispersion corrections were taken from international tables for X-ray crystallography.[31]

Density functional calculations

All calculations for Pt(DPP)(acac) were performed with Gaussian09 program package.[32a] Density functional theory B3LYP[32b,c] including Becke's three-parameter-exchange functional and the Lee–Young–Parr correlation functional was used for optimizations of the geometries of the ground state, with the standard 6-31+G(d) basis sets for C, H, O and N, and LANL2DZ[32d–f] for Pt. Following the optimizations, time dependent density functional theory (TDDFT) calculations at the B3LYP/6-31+G(d)/LANL2DZ level were carried out to evaluate the UV-Vis absorption spectrum. At the same level, the

geometry of the first excited triplet (T1) state are optimized to investigate phosphorescence emission.

Physical measurements

^{1}H NMR spectra were measured using a Bruker ARX-300 (300 MHz) spectrometer, using TMS as the internal standard. Mass spectra (MS) were measured using a VG-ZAB-HS spectrometer with electron impact ionization. Elemental analysis was performed using a PerkineElmer 240C elemental analyzer. Infrared spectra were recorded using a Bruker Vector 22 with KBr pellet. The UV-Vis spectra were recorded using a VARIAN Cary 5000 spectrometer. Phosphorescence spectra were recorded using a PerkineElmer LS 50B luminescence spectrophotometer. Quantum efficiency measurements were carried out using an optically diluted CH_3CN solution (OD < 0.05 at the excitation wavelength) and calibrated with degassed (ppy)-Pt(acac) in 2-methyltetrahydrofuran (Φ_{em} = 0.15) as a reference.[33] Eqn (1) was used to calculate quantum yields,

$$\Phi_s = \Phi_r \frac{\eta_s^2 A_r I_s}{\eta_r^2 A_s I_r} \quad (1)$$

where Φ_s is the quantum yield of the sample, Φ_r is the quantum yield of the reference, η is the refractive index of the solvent, A_s and A_r are the absorbance of the sample and the reference at the wavelength of excitation, and I_s and I_r are the integrated areas of emission bands.

Electrochemical measurements were performed using the CH Instruments model 660D electrochemical workstation. Anhydrous CH_3CN was used as the solvent and 0.1 M Bu_4NPF_6 was used as the supporting electrolyte. A three-electrode system was employed with platinum wire as the auxiliary electrode, Ag/Ag^+ as the reference electrode, and a Au disk (2 mm diameter) as the working electrode. The working electrodes were polished with 0.3 and 0.05 μm alumina slurry to obtain a mirror surface and then solicited and thoroughly rinsed with ultrapure deionized water. To eliminate the influence of oxygen, all solutions were deaerated by the bubbling of high-purity (99.995%) nitrogen. All potentials reported were against the SCE reference with the argotic system using ferrocene as an internal standard ($E^{\circ}_{Fc/Fc+}$ = 0.424 V *vs.* SCE).[34] The ECL signals were measured using the ECL analysis system for the multi-detector and an Electrochemical Analyzer (Xi'an ruimai Analytical Instruments Co., Ltd.) at room temperature. The Au disk (2 mm diameter) was employed as working electrode. The relative ECL efficiencies of Pt(DPP)(acac) and Pt(BPP)(acac) were estimated by comparing the integrated light intensity of the present system to that of the $Ru(bpy)_3^{2+}$ system under identical experimental conditions, and the electrical charges through the complexes and standard system were taken as the same. ECL efficiency (Φ_{ECL}) was obtained according to eqn (2),

$$\Phi_{ECL} = \Phi_r \frac{I_s}{I_r} \quad (2)$$

where Φ_r is the ECL efficiency of $Ru(bpy)_3^{2+}$ (taken as 1 since the absolute value of the $Ru(bpy)_3^{2+}$ efficiencies are difficult to determine[10,35]), I_s and I_r are the integrated ECL intensities of the Pt complexes and the reference $Ru(bpy)_3^{2+}$ under the same conditions, respectively.

Results and discussion

Synthesis and characterization

As depicted in Scheme 1, the required cyclometalated DPP and BPP ligands were synthesized by a reaction of the corresponding aracylpyridinium bromide, cinnamaldehyde and ammonium acetate in glacial acetic acid with moderate yields.[27,28] The platinum(II) complexes were prepared by a conventional two-step method according to the literature.[36] Treatment with K_2PtCl_4 in a mixture of 2-ethoxyethanol and H_2O gave dichloro-bridged orthometalated dimers. Subsequent treatment of the corresponding dimers with the ancillary acetylacetone ligand in the presence of a base yielded the desired platinum(II) complexes upon purification by column chromatography and crystallization. The obtained complexes were satisfactorily characterized by ^{1}H NMR, elemental analysis, IR and mass spectroscopy, and Pt(DPP)(acac) was also characterized by X-ray crystallography.

A single crystal of Pt(DPP)(acac) was grown from a dichloromethane/isobutyl alcohol solution and characterized using X-ray crystallography. A summary of the key crystallographic data and structural refinements for the complex is presented in Table 1. Selected bond distances and angles are illustrated in Table 2. The molecular structure of the complex with the atomic numbering scheme is shown in Fig. 1. The complex crystallizes in the monoclinic space group $P2_1/c$. The molecules pack as head-to-tail dimers, each molecule of the dimer related to the other by a center of inversion. The dimers have a

Table 1 Crystal data and structure refinement information of the complex Pt(DPP)(acac)

Formula	$C_{22}H_{19}NO_2Pt$
Fw	524.47
Crystal system	Monoclinic
Space group	$P2_1/c$
T (K)	298.15
a (Å)	12.6018(15)
b (Å)	11.4459(14)
c (Å)	13.9239(17)
α (°)	90
β (°)	111.159(2)
γ (°)	90
V (Å^3)	1873.0(4)
Z	4
D_c (g cm^{-3})	1.86
M (mm^{-1})	7.507
Crystal size (mm)	0.32 × 0.26 × 0.24
θ range (°)	3.46–52
Reflections collected	10 048
Unique reflections	3678
Data/parameters	3678/237
GOF on F^2	1.061
R^a, wR^b (all data)	0.0654, 0.1087
R^a, wR^b [$I > 2\sigma(I)$]	0.0458, 0.1050

$^a R = \sum||F_o| - |F_c||/\sum|F_o|$. ^{b} w$R = [\sum w(F_o^2 - F_c^2)/\sum w(F_o^2)^2]^{1/2}$.

Table 2 Selected bond lengths (Å) and angles (°) for the complex

Pt(1)–O(1)	2.001(6)	Pt(1)–N(1)	1.965(7)
Pt(1)–O(2)	2.098(7)	Pt(1)–C(1)	1.963(10)
C(1)–C(2)	1.342(13)	C(1)–C(6)	1.456(13)
C(1)–Pt(1)–O(1)	92.6(3)	O(1)–Pt(1)–O(2)	92.0(2)
C(1)–Pt(1)–N(1)	82.7(4)	C(1)–Pt(1)–O(2)	175.3(3)
N(1)–Pt(1)–O(2)	92.8(3)	N(1)–Pt(1)–O(1)	175.2(3)

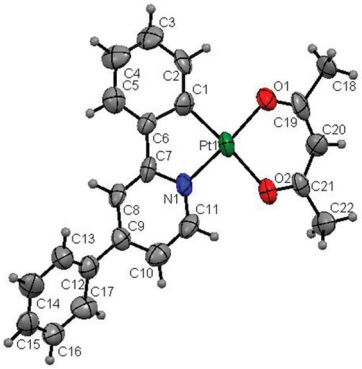

Fig. 1 ORTEP diagram of the complex Pt(DPP)(acac) showing the atom labeling scheme.

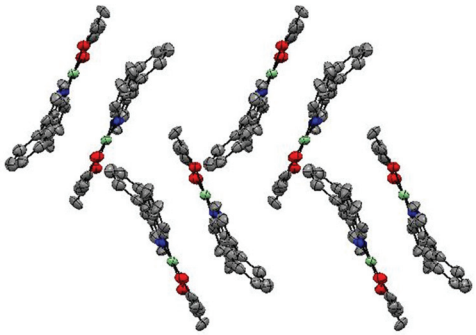

Fig. 2 ORTEP diagram showing π–π stacking of the complex.

plane-to-plane separation of 3.333 Å indicative of moderate π–π stacking interactions (Fig. 2). The distance between the pyridine ring centroid and Pt is 3.585 Å which is indicative of ring–metal interactions (Fig. 3). There are no metal–metal interactions, the closest Pt–Pt distance being 4.683 Å. The central ion Pt(II) is four-coordinated by two oxygen atoms from acac, one nitrogen atom and one carbon atom from the DPP ligand. All coordinated bond lengths (Table 2) show normal values and are comparable to those in the related cyclometalated Pt(II) complexes.[36–39] The C(1)–C(2) bond length (1.34 Å) is shorter than the normal benzene ring C–C bond length, while the C(1)–C(6) bond length (1.46 Å) is longer than normal benzene ring C–C bond length. This is due to the coordination of C(1) with the Pt(II) ion. The coordination geometry around Pt is best described as square planar, with the sum of the angles C(1)–Pt(1)–O(1), O(1)–Pt(1)–O(2), C(1)–Pt(1)–N(1) and

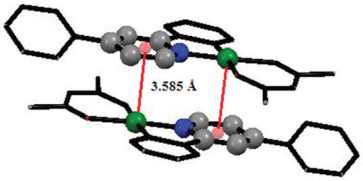

Fig. 3 The dimer of the complex showing ring–metal interaction.

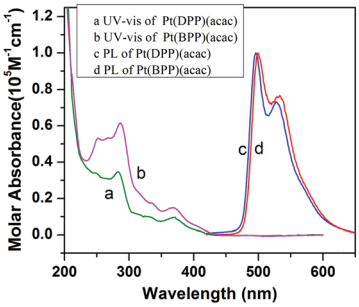

Fig. 4 The UV-Vis absorption and photoluminescence spectra of Pt(DPP)(acac) and Pt(BPP)(acac) (10^{-5} M) in CH_3CN at room temperature. Excitation wavelengths: 289 nm for Pt(DPP)(acac) and 320 nm for Pt(BPP)(acac).

N(1)–Pt(1)–O(2) being 360.1°. In the complex, DPP is a bidentate ligand which forms a stable five-membered ring. Three aromatic rings are essentially planar, and the dihedral angles between pyridine and the two benzene rings are 2.5(4) and 31.0(5)°, respectively. In addition, intramolecular C(11)–H(11)···O(2) [C···O = 2.99(1) Å] hydrogen bonding exists in the complex.

Absorption and fluorescent emission

The absorption spectra along with phosphorescence emission spectra of the complexes Pt(DPP)(acac) and Pt(BPP)(acac) were recorded at room temperature (shown in Fig. 4), and the data are summarized in Table 3. The two complexes have similar electronic absorption spectra. Low energy transitions in the absorption spectrum between 300 and 400 nm are assigned as metal-to-ligand charge transfer (MLCT) transitions and, to a certain extent, the intra-ligand state (IL), as already observed for comparable compounds.[16,36,40–42] The intense bands (ε = 3.4–6.2 × 10^4 M^{-1} cm^{-1}) observed at higher energy 200–300 nm can be described as spin-allowed, ligand-centered (LC) π→π* in nature. The two complexes show a strong green emission in CH_3CN at room temperature, with nearly identical emission spectra. This is attributed to the presence of an excited-state resulting from the mixing of comparable percentages of ^{3}LC and ^{3}MLCT states, which is in agreement with Thompson's work concerning analogous platinum complexes.[36] Strong spin–orbit coupling of central metal atoms facilitates the spin-forbidden ^{3}MLCT transitions of the metal complexes. The average value of *ca.* 500 nm for the emission maxima is red

Table 3 Absorption and emission data of Pt(DPP)(acac) and Pt(BPP)(acac)

Complex	λ_{abs}/nm[a]($\varepsilon \times 10^{-4}$/M^{-1} cm^{-1})	λ_{em}/nm	Φ_{em}[b]
Pt(DPP)(acac)	248(3.4), 283(3.5), 334(0.96), 370(0.98)	495, 527	0.17
Pt(BPP)(acac)	251(5.3), 268(5.3)286(6.2), 334(1.8), 368(1.5)	499, 533	0.21

[a] Absorption measurements of the complexes were carried out in anhydrous CH_3CN. [b] Values obtained in thoroughly degassed CH_3CN using degassed (ppy)Pt(acac) in 2-methyltetrahydrofuran (Φ_{em} = 0.15) as a reference.

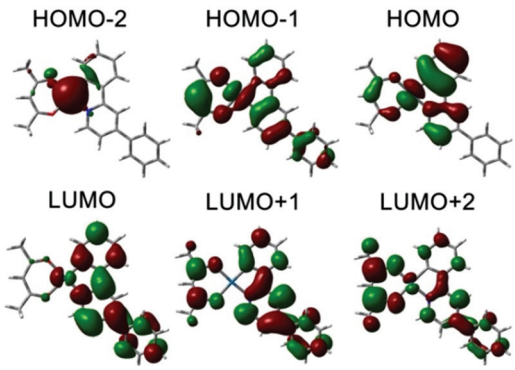

Fig. 5 Contour plots of the three highest occupied molecular orbitals (HOMOs) and the three lowest unoccupied molecular orbitals (LUMOs) of complex Pt(DPP)(acac).

shifted by *ca.* 20 nm from that of the similar complex [Pt(ppy)-(acac)]. This is due to the enlarged conjugation system of the ligands and corresponds to the lower π^* orbital (LUMO) energy of the substituted phenylpyridine ligand compared to that of the ppy ligand which results in a decrease in the energy gap between HOMO and LUMO.

The introduction of the *t*-butyl group makes the Φ_{em} of Pt-(BPP)(acac) higher than that of Pt(DPP)(acac), which is proposed to be due to a decrease of self-quenching. It is noteworthy that both of the Φ_{em} for the synthesized complexes, 0.19 for Pt(DPP)(acac) and 0.21 for Pt(BPP)(acac), are substantially greater than that of $Ru(bpy)_3^{2+}$ (Φ_{em} = 0.095 in CH_3CN[43]).

DFT calculations

Density functional theory (DFT) and time dependent DFT (TDDFT) calculations are performed to investigate the photophysical properties of the complex Pt(DPP)(acac). B3LYP and cam-B3LYP functionals were both tested with the standard 6-31+G(d) basis sets for the light elements and LANL2DZ for Pt. The results obtained at the B3LYP/6-31+G(d)/LANL2DZ level reproduced the UV-VIS absorption spectrum better than using cam-B3LYP, thus in the following discussion, only the B3LYP results will be discussed. Some features of the important frontier orbitals are displayed in Fig. 5. The transition from T_1 to S_1 state is mainly contributed with the LUMO → HOMO (72.7%) transition. The HOMO consists of a mixture of the phenyl from DPP (54.7%), Pt (33.6%), and acac (11.7%) orbitals, while the LUMO is predominantly DPP (93.5%) in character. The results clearly indicate that the observed emission has mostly LC character with a mixture of MLCT. The calculated phosphorescence line from $T_1 \rightarrow S_0$ is at 544 nm, which is in good agreement with the experimental measured emission energies.

Electrochemistry and electrochemiluminescence

The electrochemical properties of the complexes were determined by cyclic voltammetry (CV) using Bu_4NPF_6 (0.1 M) as the supporting electrolyte in anhydrous CH_3CN solution. All electrochemical data *vs.* SCE for the two complexes are collected in Table 4. Both of the complexes described here show a quasi-reversible reduction wave at −1.80 V *vs.* SCE, an irreversible reduction wave at about −2.30 V, and irreversible oxidation wave near 0.75 V (shown in Fig. 6). It is generally considered that the oxidation of this species can be mainly attributed to the metal center, with a substantial contribution from the ligands. Since square planar Pt(I) and Pt(II) metal centers are susceptible to nucleophilic attack by solvents, the Pt(II) redox processes are usually irreversible.[44] The reduction process are mainly localized on the *C*^*N* ligands, with only a partial contribution from the metal center.[45]

The ECL performances of the complexes using a 10 μM sample were studied in CH_3CN, DMF and CH_2Cl_2, respectively, and the results are collected in Table 4. A stable ECL of the

Table 4 Electrochemical and ECL properties of the complexes

	Electrochemistry (V *vs.* SCE)[a]			Electrochemiluminescence				
				Rel Φ_{ECL}[c]			Coreactant System (TPrA) Rel Φ_{ECL}[e]	
Complex	E_{pa}^{Oxd}	$E_{1/2}^{Red}$[b]		CH_3CN	DMF	CH_2Cl_2	CH_3CN	CH_3CN–PBS (50 : 50, V)
Pt(DPP)(acac)	+ 0.79	−1.77	−2.26	0.19	[d]	[d]	0.87	0.86
Pt(BPP)(acac)	+ 0.75	−1.79	−2.29	0.21	[d]	[d]	0.91	0.89

[a] All potentials were determined at room temperature in deaerated DMF solutions (0.1 M Bu_4NPF_6) *vs.* SCE at scan rate of 100 mV s^{-1}. [b] $E_{1/2}$ refers to [(E_{pa} + E_{pc})/2] where E_{pa} and E_{pc} are the anodic and cathodic peak potentials. [c] Φ_{ECL} were calculated with respect to the ECL efficiency of $Ru(bpy)_3^{2+}$ and the electrical charges through the systems were taken as the same (the Φ_{ECL} of $Ru(bpy)_3^{2+}$ was taken as 1) in CH_3CN. [d] Too weak to be measured. [e] Relative ECL efficiencies with respect to $Ru(bpy)_3^{2+}$/TPrA and the electrical charges through the systems were taken as the same (the Φ_{ECL} of $Ru(bpy)_3^{2+}$ was taken as 1), ECL solutions contained 10 μM complex and 25 mM TPrA. Reported values were averaged from at least five scans with a relative standard deviation of ~7%.

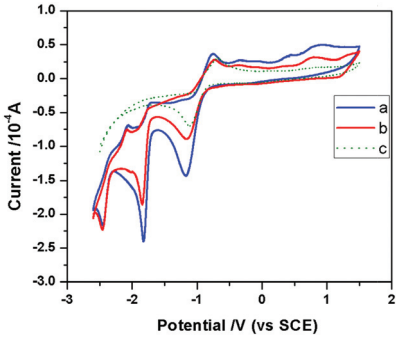

Fig. 6 Successive cyclic voltammograms of the complexes (1 mM) in anhydrous CH_3CN containing 0.1 M Bu_4NPF_6 as the supporting electrolyte at the Au disk electrode. Scan rate, 100 mV s^{-1}. (a) Pt(DPP)(acac); (b) Pt(BPP)(acac); (c) the blank cyclic voltammogram in CH_3CN containing 0.1 M Bu_4NPF_6 under the same experimental conditions.

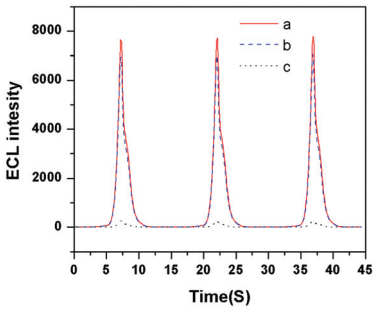

Fig. 7 ECL intensity-time curves of 10 μM Pt(DPP)(acac), scanning voltage range from 0.0 to 0.80 V. (a) in CH_3CN solution containing 25 mM TPrA and 0.1 M Bu_4NPF_6 (b) in CH_3CN–PBS (PH = 7.5, 50 : 50 ,V) and (c) in CH_3CN solution containing 0.1 M Bu_4NPF_6.

complex Pt(DPP)(acac) and Pt(BPP)(acac) solution containing 0.1 M Bu_4NPF_6 was observed in CH_3CN when the potential of the Au working electrode was pulsed from 0 to 1.5 V (Fig. 7(c) for Pt(DPP)(acac) as an example), while in DMF and CH_2Cl_2 media, the ECL emission of the two complexes is unobserved or very weak, which indicates that DMF and CH_2Cl_2 can intensively quench the ECL emission. Therefore, the following investigation for ECL of the two complexes was carried out in CH_3CN solution. The ECL intensity peaks of the complex Pt(DPP)(acac) and Pt(BPP)(acac) appear at potentials of 1.19 and 1.20 V *vs.* SCE, respectively, as shown in Fig. 8(A). Compared with that of $[Ru(bpy)_3]^{2+}$, the potential for a redox couple of the two complexes is shifted by ~0.26 V towards a more negative potential.

The coreactant system ECL also has been studied using a 10 μM sample of the complexes in CH_3CN at the Au working electrode with TPrA as the coreactant. A significant increase of the ECL signal of the two complexes was observed in presence of TPrA, as listed in Fig. 7(a) taking the complex Pt(DPP)(acac) as an example. When the potential is scanned from 0 to 1.5 V for 10 times, the ECL signals of the Pt(DPP)(acac) and Pt(BPP)-(acac)/TPrA systems are almost unchanged, indicating these new ECL systems could be used as novel ECL reagents. The

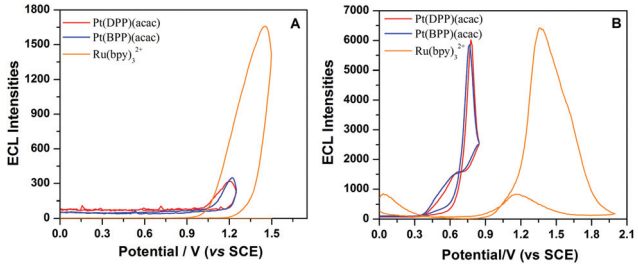

Fig. 8 ECL intensity-potential curves of 10 μM Pt(DPP)(acac), Pt(BPP)(acac) and $Ru(bpy)_3^{2+}$ in CH_3CN containing 0.1 M Bu_4NPF_6; (A) in the absence of TPrA; (B) in the presence of 25 mM TPrA.

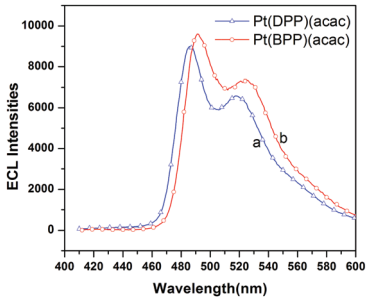

Fig. 9 ECL spectra of the complexes using a 10 μM sample in deaerated CH_3CN solution: Bu_4NPF_6 as supporting electrolyte, TPrA as oxidative reductive co-reactant, scan range: 0–1.5 V.

ECL spectra of the complexes were quite similar to their own emission spectrum obtained on photoexcitation (Fig. 9 and 4), indicating that the same ^{3}MLCT states are probably formed in both experiments.[21,46] The ECL intensity peaks of the complex Pt(DPP)(acac) and Pt(BPP)(acac) with TPrA as the coreactant appear at potentials of 0.76 and 0.77 V *vs.* SCE, respectively, as shown in Fig. 8(B). Compared with that of $[Ru(bpy)_3]^{2+}$/TPrA, the potential for a redox couple of the two complexes is shifted by ~0.6 V towards a more negative potential. A lower redox potential is helpful to decrease background interference. The potentials of the maximum ECL intensity of the Pt(BPP)(acac)/TPrA system are slightly shifted by about 0.01 V towards a more negative potential compared with those of the Pt(DPP)-(acac)/TPrA system, which is consistent with that obtained by cyclic voltammogram scans.

It is found that the ECL intensities of Pt(DPP)(acac) and Pt(BPP)(acac) in CH_3CN depend on the concentration of the coreactant. As shown in Fig. 10, the ECL intensities of the two complexes noticeably increase with an increase in the concentration of TPrA up to 25 mM and then decrease slowly upon a further increase of the TPrA concentration. The ECL intensity changes of the two complexes with different TPrA concentrations are in agreement with those found in the $[Ru(bpy)_3]^{2+}$/TPrA coreactant system.[47,48]

To further estimate whether these types of compounds can be applied in immunoassays and DNA analysis, the ECL performances in mixed CH_3CN–H_2O (50 : 50, v/v) solutions were also studied. Strong and stable ECL appeared as observed

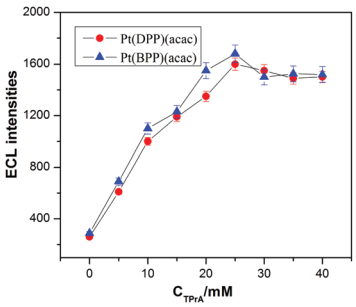

Fig. 10 ECL intensity changes of 10 μM Pt(DPP)(acac) or Pt(BPP)(acac) with different concentrations of the TPrA coreactant at a Au working electrode.

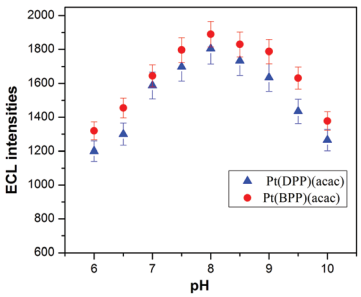

Fig. 11 ECL intensity changes of 10 μM Pt(DPP)(acac) or Pt(BPP)(acac) with different pH at a Au working electrode. TPrA (25 mM) in 0.10 M PBS solution (50% MeCN). Scan rate, 100 mV s^{-1}.

in pure CH_3CN (listed in Fig. 7(b)) with only a slight decrease. The ECL emission is also pH dependent in 50 : 50 (v/v) CH_3CN–PBS solutions, and maximum intensities were observed at pH ~8 for Pt(DPP)(acac) and Pt(BPP)(acac) (shown in Fig. 11). Similar trends are observed for the $Ru(bpy)_3^{2+}$ coreactant system.[4,49] This is important for potential applications since the pH of the environmental and biological systems is ~7.4 and would require less sample preparation prior to analysis. It also suggests that both ruthenium- and platinum-based complexes can be used in the same sample solution for multi-analyst ECL determination.

The ECL quantum efficiencies of the Pt(DPP)(acac) and Pt(BPP)(acac)/TPrA coreactant systems in different media were measured using $Ru(bpy)_3^{2+}$/TPA (Φ_{ECL} was taken as 1) as the standard, and the data were given in Table 4. Under the same experimental conditions, the ECL quantum efficiency of Pt(BPP)(acac) (Rel Φ_{ECL} = 0.91) is slightly higher than that of Pt(DPP)(acac) (Rel Φ_{ECL} = 0.87), which are comparable to that of the $Ru(bpy)_3^{2+}$/TPrA system.

ECL mechanism

It is clear from Fig. 4 and 9 that the ECL spectra of the complexes/TPrA system are almost identical with their PL spectra, indicating that the excited state obtained on photoexcitation is also generated in the ECL experiment. By analogy with the well-known $Ru(bpy)_3^{2+}$ system and other platinum(II) complexes,[21,50] in the absence of the redox coreactant, the generation of luminescence from Pt complexes solutions on pulsing the potential from −2.0 to 1.25 V can be explained by the following reactions:

$$Pt + e^- \rightarrow Pt^{-\cdot} \quad (3)$$

$$Pt - e^- \rightarrow Pt^{+\cdot} \quad (4)$$

$$Pt^{-\cdot} + Pt^{+\cdot} \rightarrow Pt* + Pt \quad (5)$$

$$Pt* \rightarrow Pt + h\nu \quad (6)$$

where Pt represents the Pt(DPP)(acac) or Pt(BPP)(acac) complex. When TPrA is employed as a coreactant, the emitter complex (Pt) is oxidized to $Pt^{+\cdot}$ at an electrode and then interacts with $TPrA^{\cdot}$, which is irreversibly generated by the oxidation and decomposition of TPrA at the electrode, to receive an electron and forms an excited-state species, as shown in the following reaction sequences:

$$Pt - e^- \rightarrow Pt^{+\cdot} \quad (4)$$

$$TPrA - e^- \rightarrow TPrA^{+\cdot} \quad (7)$$

$$TPrA^{+\cdot} \rightarrow TPrA^{\cdot} + H^+ \quad (8)$$

$$TPrA^{\cdot} + Pt^{+\cdot} \rightarrow Pt* + TPrA \quad (9)$$

$$Pt* \rightarrow Pt + h\nu \quad (10)$$

In the coreactant system, the intense ECL is ascribed to the strong reducing power of $TPrA^{\cdot}$ ($E(TPrA^{\cdot})$ = −1.7 V), reducing $Pt^{+\cdot}$ directly into Pt*.[51] The generated cation radicals of $TPrA^{\cdot +}$ (eqn (5)) play key roles in light emission since the deprotonation process of $TPrA^{\cdot +}$ to $TPrA^{\cdot}$ (eqn (7)) can occur extremely quickly and the oxidation of the emitter complexes (eqn (2)) could occur relatively fast.

Conclusions

Two neutral cyclometalated platinum(II) complexes bearing a substituted 2-phenylpyridine and a β-diketone, have been synthesized and characterized. The photophysical and electrochemical behaviors have been investigated. The ECL characteristics in the absence or presence of coreactant TPrA in different solvents have also been investigated. Stable and intense ECL for the Pt(II) complexes has been observed with TPrA as a coreactant at reasonable voltage and pH levels. The ECL potentials of Pt(DPP)(acac) and Pt(BPP)(acac) in CH_3CN and CH_3CN/H_2O solution were at ~0.75 V *vs.* SCE, and significantly negatively shifted by about 0.6 V compared to that of the $Ru(bpy)_3^{2+}$/TPrA system. Moreover, the ECL quantum efficiency of Pt(BPP)(acac) is slightly higher than that of Pt(DPP)(acac) and approximates to that of the $Ru(bpy)_3^{2+}$/TPrA system. The fact that the electrochemical and ECL behavior of the Pt(II) complexes are very similar to those of $Ru(bpy)_3^{2+}$/TPrA indicates that the synthesized Pt(II) complexes can be an alternative for conventional $Ru(bpy)_3^{2+}$ complexes. They could be used as novel ECL luminophores which are used in many

interesting fields, particularly for those demanding specific biological activities in water.

Acknowledgements

This work was financially supported by the Natural Science Foundation of China (No. 21205065 and 20971076), Postdoctoral Science Foundation of China (2012M521371) and the Natural Science Foundation of Shandong Province (No. ZR2010BZ006 and ZR2009BM019).

Notes and references

1 M. M. Richter, *Chem. Rev.*, 2004, **104**, 3003.
2 W. J. Miao, *Chem. Rev.*, 2008, **108**, 2506.
3 *Electrogenerated Chemiluminescence*, ed. A. J. Bard, Marcel Dekker, New York, 2004.
4 B. D. Muegge and M. M. Richter, *Anal. Chem.*, 2002, **74**, 547.
5 N. Tokel and A. J. Bard, *J. Am. Chem. Soc.*, 1972, **94**, 2862.
6 V. Balzani and A. Juris, *Coord. Chem. Rev.*, 2001, **211**, 97.
7 S. G. Sun, Y. Yang, F. Y. Liu, Y. Pang, J. L. Fan, L. C. Sun and X. J. Peng, *Anal. Chem.*, 2009, **81**, 10227.
8 E. M. Gross, J. D. Anderson, A. F. Slaterbeck, S. Thayumanavan, S. Barlow, Y. Zhang, S. R. Marder, H. K. Hall, M. F. Nabor, J. F. Wang, E. A. Mash, N. R. Armstrong and R. M. Wightman, *J. Am. Chem. Soc.*, 2000, **122**, 4972.
9 Q. H. Wei, F. N. Xiao, L. J. Han, S. L. Zeng, Y. N. Duan and G. N. Chen, *Dalton Trans.*, 2011, **40**, 5078.
10 J. I. Kim, I. S. Shin, H. Kim and J. K. Lee, *J. Am. Chem. Soc.*, 2005, **127**, 1614.
11 H. D. Abruna, *J. Electroanal. Chem.*, 1984, **175**, 321–325.
12 Z. F. Chen, K. M. C. Wong, E. C. H. Kwok, N. Y. Zhu, Y. B. Zu and V. W. W. Yam, *Inorg. Chem.*, 2011, **50**, 2125.
13 V. H. Houlding and V. M. Miskowski, *Coord. Chem. Rev.*, 1991, **111**, 145.
14 C. Yu, K. M. C. Wong, K. H. Y. Chan and V. W. W. Yam, *Angew. Chem., Int. Ed.*, 2005, **44**, 791.
15 E. Shikhova, E. O. Danilov, S. Kinayyigit, I. E. Pomestchenko, A. D. Tregubov, F. Camerel, P. Retaileau, R. Ziessel and F. N. Castellano, *Inorg. Chem.*, 2007, **46**, 3038.
16 B. W. Ma, J. Li, P. I. Djurovich, M. Y. Robert Bau and M. E. Thompson, *J. Am. Chem. Soc.*, 2005, **127**, 28.
17 M. Oyama and S. Okazaki, *Anal. Chem.*, 1998, **70**, 5079.
18 A. Vacher, F. Barrière, F. Camerel, J.-F. Bergamini, T. Roisnel and D. Lorcy, *Dalton Trans.*, 2013, **42**, 383.
19 V. W. W. Yam, R. P. L. Tang, K. M. C. Wong and K. K. Cheung, *Organometallics*, 2001, **20**, 4476.
20 K. M. C. Wong, W. S. Tang, B. W. K. Chu, N. Zhu and V. W. W. Yam, *Organometallics*, 2004, **23**, 3459.
21 S. Bonafede, M. Ciano, F. Bolletta, V. Balzani, L. Chassot and A. Zelewsky, *J. Phys. Chem.*, 1986, **90**, 3836.
22 C. A. Strassert, C.-H. Chien, M. D. Galvez Lopez, D. Kourkoulos, D. Hertel, K. Meerholz and L. D. Cola, *Angew. Chem., Int. Ed.*, 2011, **50**, 946.
23 A. Y.-Y. Tam, K. M.-C. Wong and V. W.-W. Yam, *J. Am. Chem. Soc.*, 2009, **131**, 6253.
24 M. Mydlak, M. Mauro, F. Polo, M. Felicetti, J. Leonhardt, G. Diener, L. D. Cola and C. A. Strassert, *Chem. Mater.*, 2011, **23**, 3659.
25 C.-C. Kwok, H. M. Y. Ngai, S.-C. Chan, I. H. T. Sham, C.-M. Che and N. Zhu, *Inorg. Chem.*, 2005, **44**, 4442.
26 R. Liu, H. B. Chen, J. Chang, Y. H. Li, H. J. Zhu and W. F. Sun, *Dalton Trans.*, 2013, **42**, 160.
27 F. Krohnke, *Synthesis*, 1976, 1.
28 P. P. Sun, C. X. Li, Y. Pan and Y. Tao, *Synth. Met.*, 2006, **156**, 525.
29 B. N. Cockburn, D. V. Howe, T. Keating, B. F. G. Johnson and J. Lewis, *J. Chem. Soc., Dalton Trans.*, 1973, 404.
30 G. M. Sheldrick, *Acta Crystallogr., Sect. A: Found. Crystallogr.*, 2008, **64**, 112.
31 A. J. C. Wilson, *International Tables for X-ray Crystallography*, Kluwer Academic Publishers, Dordrecht, 1992, vol. C; Tables 6.1.1.4 (pp. 500–520) and 4.2.6.8 (pp. 219–222), respectively.
32 (*a*) M. J. Frisch, G. W. Trucks, H. B. Schlegel, *et al.*, *GAUSSIAN 09, (Revision B.01)*, Gaussian, Inc., Wallingford CT, 2010; (*b*) C. Li, W. Yang and R. G. Parr, *Phys. Rev. B*, 1988, **37**, 785; (*c*) A. D. Becke, *J. Chem. Phys.*, 1993, **98**, 5648; (*d*) P. J. Hay and W. R. Wadt, *J. Chem. Phys.*, 1985, **82**, 270; (*e*) W. R. Wadt and P. J. Hay, *J. Chem. Phys.*, 1985, **82**, 284; (*f*) P. J. Hay and W. R. Wadt, *J. Chem. Phys.*, 1985, **82**, 299.
33 H. S. White and A. J. Bard, *J. Am. Chem. Soc.*, 1982, **104**, 6891.
34 R. R. Gagné, C. A. Koval and G. C. Lisensky, *Inorg. Chem.*, 1980, 19.
35 (*a*) M. M. Richter, J. D. Debad, D. R. Striplin, G. A. Crosby and A. J. Bard, *Anal. Chem.*, 1996, **68**, 4370; (*b*) B. D. Muegge and M. M. Richter, *Anal. Chem.*, 2004, **76**, 73.
36 J. Brooks, Y. Babayan, S. Lamansky, P. I. Djurovich, I. Tsyba, R. Bau and M. E. Thompson, *Inorg. Chem.*, 2002, **41**, 3055.
37 J. Breu, K.-J. Range, A. Von Zelewsky and H. Yersin, *Acta Crystallogr.*, 1997, 562.
38 M. Ghedini, D. Pucci, A. Crispini and G. Barberio, *Organometallics*, 1999, **18**, 2116.
39 M. Katoh, K. Miki, Y. Kai, N. Tanaka and N. Kasai, *Bull. Chem. Soc. Jpn.*, 1981, **54**, 611.
40 P. Shao, Y. Li, A. Azenkeng, M. R. Hoffmann and W. Sun, *Inorg. Chem.*, 2009, **48**, 2407.
41 J. DePriest, G. Y. Zheng, N. Goswami, D. M. Eichhorn, C. Woods and D. P. Rillema, *Inorg. Chem.*, 2000, **39**, 1955.
42 K. P. Balashev, M. V. Puzyk, V. S. Kotlyar and M. V. Kulikova, *Coord. Chem. Rev.*, 1997, **159**, 109.

43 K. Suzuki, A. Kobayashi, S. Kaneko, K. Takehira, T. Yoshihara, H. Ishida, Y. Shiina, S. Oishic and S. Tobita, *Phys. Chem. Chem. Phys.*, 2009, **11**, 9850.
44 P.-I. Kvam, M. V. Puzyk and K. P. Balashev, *Acta Chem. Scand.*, 1995, **49**, 335.
45 M. V. Kulikova, K. P. Balashev and P.-I. Kvam, *J. Russ. J. Gen. Chem.*, 2000, **70**, 163.
46 Q. H. Wei, , L. J. Han, , Y. Jiang, , X. X. Lin, , Y. N. Duan and and G. N. Chen, *Inorg. Chem.*, 2012, **51**, 11117.
47 W. J. Miao and A. J. Bard, *Anal. Chem.*, 2003, **75**, 5825.
48 M. Zhou, G. P. Robertson and J. Roovers, *Inorg. Chem.*, 2005, **44**, 8317.
49 I. Rubinstein and A. J. Bard, *J. Am. Chem. Soc.*, 1981, **103**, 512.
50 N. E. Tokel-Takvoryan, R. D. Hemingway and A. J. Bard, *J. Am. Chem. Soc.*, 1973, **95**, 6582.
51 R. Y. Lai and A. J. Bard, *J. Phys. Chem. A*, 2003, **107**, 3335.